Tellus (1991), *43AB*, 104–115

Poleward heat transport in the ocean
A review of a hierarchy of models of increasing resolution

By KIRK BRYAN, *Geophysical Fluid Dynamics Laboratory/NOAA, Princeton, New Jersey 08542, USA*

(Manuscript received 10 September 1990; in final form 12 February 1991)

ABSTRACT

The large-scale transport of heat and carbon by the ocean circulation play an important role in the Earth's climate. Progress in developing realistic models of this process is reviewed. Sufficient numerical experiments have been carried out to indicate the role of subgrid scale mixing of temperature and salinity in the transport behavior of the models. The vertical component of subgrid diffusion in the models is essential for determining the amplitude of the thermohaline circulation of the ocean. In the case of simple geometries, poleward heat transport in models is approximately proportional to vertical mixing to the two-thirds power. The horizontal component of the diffusion appears to play almost no role in the poleward transport of heat as long as the value is less than 10^3 m^2/s. At low values of horizontal diffusion and viscosity, mesoscale eddies are generated spontaneously in the models through baroclinic and barotropic instability. In analogy with the atmosphere one would expect these mesoscale disturbances to play an important role in poleward heat transport. The results of numerical experiments show that this may not be the case. The mesoscale eddies in the models generate mean flows which tend to cancel the eddy fluxes in much the same way that eddy-mean flow compensation occurs for atmospheric disturbances in the lower stratosphere.

1. Introduction

Broadly speaking, the main components of the climate system are the atmosphere, ocean, land hydrology and the biosphere. Progress in understanding the Earth's climate in all its complexity depends on the availability of credible models of each of these components of the system. The existence of such models is a prerequisite for the careful study of the complex interactions of climate. It is also essential to provide the insights needed for projecting global change. The rapid progress that has been made in modelling the Earth's atmosphere suggests that a comprehensive model of the entire climate system is an ambitious, but entirely feasible goal. This paper is concerned with extending the modelling capability that now exists for the atmosphere to the ocean.

The quantitative role of the World Ocean in the global heat balance under present climatic conditions is still poorly known. We are handicapped in constructing models which will predict past and future climate conditions by a poor understanding of the present. Two principle roles of the ocean in the globel balance are well known in a qualitative sense. One is the ocean's ability to store heat, which moderates seasonal extremes and gives rise to the very obvious difference between continental and marine climates. The second important role of the oceans is to work with the atmosphere in transporting excess heat received from the sun in equatorial latitudes and transporting it to polar latitudes. At this point it is difficult to determine the exact partitioning of this poleward heat transport between the ocean and atmosphere. Some of the uncertainties are discussed by Dobson et al. (1982) "CAGE Feasibility Report". Field studies carried out in the last few decades have provided a description of the spectrum of variability of temperature and velocity in a few parts of the ocean. One of the important results of these measurements was to show that the kinetic energy of geostrophic motions in the oceans is dominated by mesoscale eddies of 100–200 km in wavelength. The kinetic energy of the time-averaged ocean circulation, itself, was only a small fraction of the

total. A diagram comparing the kinetic energy spectra of the atmosphere and ocean by Woods (1985) is shown in Fig. 1. The atmosphere has its peak kinetic energy at wavelengths of about 2000–4000 km. Part of the success of numerical weather forecasting is due to the fact that energy at larger wave numbers falls off rapidly. Thus it was possible to resolve a large part of the atmospheric spectrum in the relatively primitive computers that were available two decades ago. Note that the peak in the ocean spectrum is shifted to a much higher wavenumber, corresponding to spatial scales of 100–200 km. This is associated with the fact that the density differences in the ocean are much less than in the atmosphere. The favored wave length for synoptic disturbances corresponding to cyclones and anticyclones in the atmosphere is roughly ten times smaller in the ocean.

It is a well established fact that cyclones and anticyclones have an essential role in the general circulation of the atmosphere. This fact is often cited in support of the view that ocean models which did not explicitly resolve mesoscale eddies might have an entirely different heat and dynamical balance than those that did include these features. At this point the comprehensive models of the World Ocean and the WOCE data base are not available to test this idea. However, a series of calculations have been carried out in models of idealized geometry which increase the horizontal resolution of models from a course grid of about 400×400 km down to about 15×15 km. While a great deal of caution is required in applying the results of these physically simplified models to the ocean itself, these series of experiments do provide some very important insights on the transport processes of a system with most of the important dynamic properties of the World Ocean.

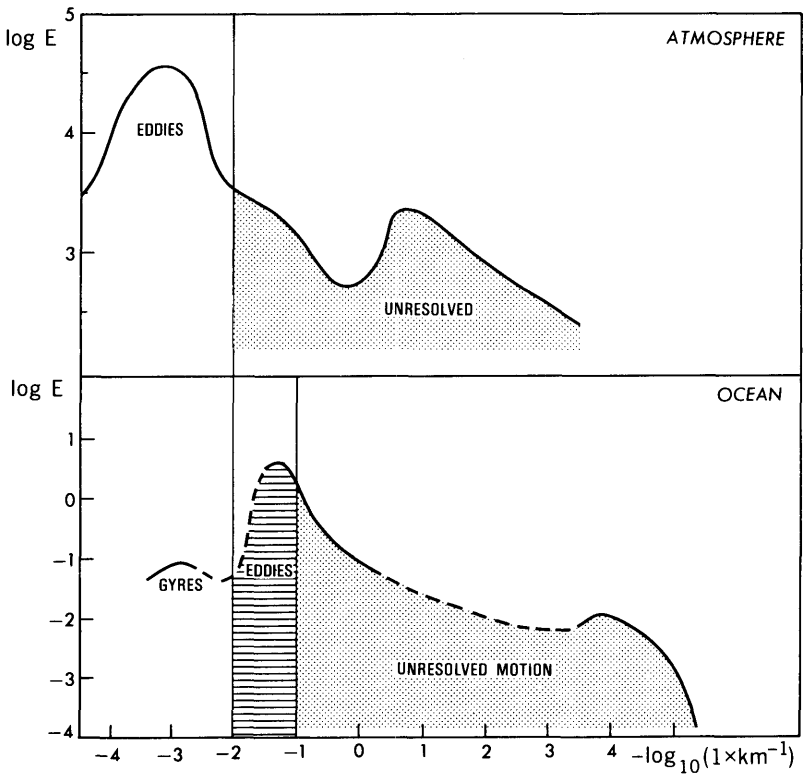

Fig. 1. The kinetic energy spectrum as a function of horizontal wave number for the atmosphere and ocean after Woods (1985). The ordinate is in units of m^2/s and the abscissa in units of cycles/km.

Examination of the poleward heat transport in this hierarchy of models of increasing resolution is the subject of this review.

2. Model equations

As a point of reference for nonspecialists, the model equations will be briefly described. The hydrostatic assumption is a standard simplification in large scale models for the ocean and atmospheric circulation. It means that all acceleration and friction terms are dropped in the vertical momentum equation, and the vertical pressure gradient is balanced only by the buoyancy force. In oceanography the Boussinesq approximation is also frequently introduced. This implies that the density is treated as a constant in the momentum equations, except where it appears in the buoyancy force term. The rigid lid approximation filters out fast-moving external gravity "tsunami" waves, and only slightly distorts the dispersion of external Rossby waves. Let $\boldsymbol{u}$ be the horizontal velocity vector, and ∇ be the horizontal gradient vector. If ρ is the density, p is the pressure, and w the vertical component of velocity, the equations of motion may be written as:

$$\mathrm{d}_t \boldsymbol{u} + 2\Omega \sin \phi \boldsymbol{k} \times \boldsymbol{u} + \frac{1}{\rho_0} \nabla p = \boldsymbol{F}, \tag{1}$$

$$\rho g + \partial_z p = 0, \tag{2}$$

where F is the forcing;

$$F = D_\mathrm{v} \partial_z \partial_z \boldsymbol{u} + D_\mathrm{H} \nabla^2 \boldsymbol{u}; \tag{3}$$

D_v and D_H are the coefficients of vertical and horizontal viscosity.

The continuity equation is

$$\partial_z w + \nabla \cdot \boldsymbol{u} = 0. \tag{4}$$

In most of the models we shall discuss, salinity is not included explicitly. Thus

$$\rho = \rho_0 (1 - \alpha \theta) \tag{5}$$

and

$$\mathrm{d}_t \theta = \partial_z K_\mathrm{v} \partial_z \theta + K_\mathrm{H} \nabla^2 \theta, \tag{6}$$

where θ is temperature. K_v and K_H are the vertical and horizontal coefficients of diffusive mixing. When salinity is included the eq. of state, (5) becomes much more complex, and must include nonlinear terms involving temperature, salinity and pressure. In that case an extra conservation equation for salinity must also be included.

Convection is taken into account in the vertical diffusion term on the right-hand side of eq. (6). If the vertical stratification ever becomes unstable as the result of cold water being advected over warmer water or through a cooling at the surface, vertical diffusion is made infinite until the stratification is restored to a neutral condition. It has been pointed out (Killworth, 1989) that the actual iterative numerical algorithm used to implement convective overturning in many recent computations does not simulate this process very accurately. As modelers become aware of this problem more exact procedures are being implemented.

Boundary conditions for the model require no normal flow through the boundaries, which include a "rigid lid" horizontal surface at the upper boundary. Gradients of temperature and salinity normal to the lateral and bottom boundaries are also required to be zero, so that water mass properties are only modified by fluxes through the upper boundary and internal fluxes within the ocean. The effect of atmospheric winds is taken into account by the flux of momentum through the upper surface.

3. The low resolution experiments of Colin de Verdière and F. Bryan

Recently, two very interesting studies have been carried out to clarify the properties of low resolution models of the ocean circulation (Bryan, 1987; Verdière, 1988, 1989). The simplified geometries of these two models are shown in Fig. 2. Both models introduce spherical geometry. Bryan's (1987) model is based on the full primitive equations as given in Section 2. A realistic equation of state is included and both temperature and salinity are treated explicitly. Zonally uniform, but realistic values of temperature, salinity and wind stress are specified at the upper surface as indicated in Fig. 2. The model of Colin de Verdière (1988) is a simple box enclosed by two meridians and two parallels of latitude at 20°N and 60°N. The dynamics of

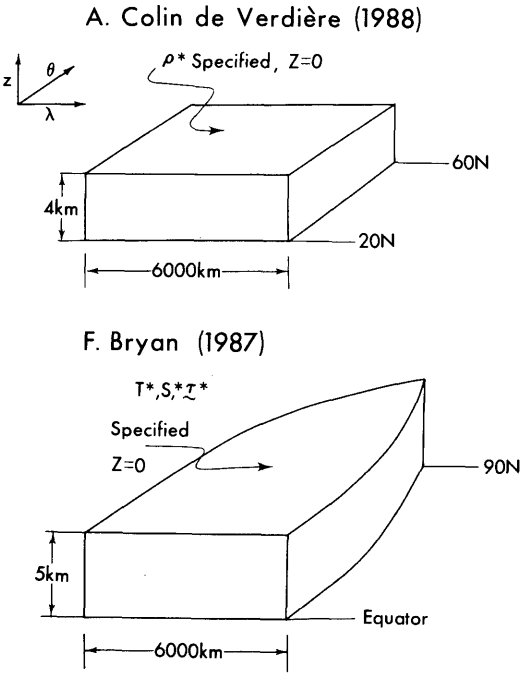

Fig. 2. Schematic diagrams showing the geometry of the numerical ocean circulation experiments of Colin de Verdière (upper panel) and F. Bryan (lower panel).

the model in this case are also simplified, omitting the local time-derivative and inertial terms in the equations of motion. This approximation is justified for a low resolution model of this kind, which is well removed from the equator. In the Colin de Verdière model temperature and salinity are not included explicitly. A single conservation equation for buoyancy specifies the mass field. All nonlinear effects in the model are represented in the equation for the buoyancy. No dynamic effects corresponding to wind stress are introduced in this particular study, but are included in a later study (Colin de Verdière, 1989). The parameters for all the numerical experiments referenced in this review are given in Table 1. A dashed line indicates that a range of values were used in a series of experiments.

Both studies show that one of the most interesting parameters of the model is the vertical diffusivity that determines the depth of the model thermocline in the absence of wind. Let V be a velocity scale and D the scale depth of the thermocline. Let g' be the acceleration of gravity reduced by the ratio of the scale difference in density imposed by the boundary conditions to the density itself. Ω is the angular velocity of the Earth, and L is a basin scale, the familiar thermal wind relation defines the velocity scale,

$$V = g'D/(2\Omega L). \tag{7}$$

A vertical scale velocity W may be defined by

$$W = DV/L. \tag{8}$$

A balance between upwelling and diffusion (Munk, 1966) on the average implies,

$$W/D = K_v/D^2. \tag{9}$$

Combining (3.1)–(3.3) gives an expression for the

Table 1. *Parameters of numerical experiments*

	Bryan (1987)	Colin de Verdière (1988)	Cox (1985) low	Cox (1985) intermediate	Böning (1991) high
$\Delta\lambda$ (degrees)	3.75	3.0	1.2	0.4	0.2
$\Delta\phi$ (degrees)	4.5	2.5	1.0	1/3	1/6
D_H (m^2/s)	2.5×10^5	6.0×10^5	10^4	(-8.0×10^{10})	(-10^{10})
D_v (m^2/s)	1.0×10^{-4}	0.0	10^{-3}	10^{-3}	10^{-3}
K_H (m^2/s)	1.0×10^3	$0.25\text{–}5.0\times10^3$	10^3	(-2.4×10^{11})	(-4.0×10^{10})
K_v (m^2/s)	-	-	0.3×10^{-4}	0.3×10^{-4}	0.3×10^{-4}

D_H = horizontal viscosity K_H = horizontal diffusivity
D_v = vertical viscosity K_v = vertical diffusivity

N.B. Numbers in parenthesis refer to coefficients of biharmonic viscosity and diffusion. The units in this case are m^4/s. Dashed lines indicate that a range of values were used.

vertical scale of the thermocline in terms of the other parameters

$$D^3 = 2\Omega L^2 K_v / g' \qquad (10)$$

Note that D, the scale depth, is proportional to the $\frac{1}{3}$ power of K_v.

A similar dependence of the scale depth of the thermocline on vertical diffusion is illustrated in the numerical experiments of Bryan and Colin de Verdière as shown in Fig. 3. Since F. Bryan's experiments include the effect of wind, Ekman pumping and Ekman suction will also influence the depth of the thermocline. The results for $K_v = 10^{-5}$ m^2/s indicate that the thermocline at latitudes 30°–10° N is much deeper than predicted by eq. (10) due to Ekman pumping in the subtropical gyre. At 40° N, the results are not effected as much because this latitude is on the boundary between the wind gyres.

Estimates of the poleward heat transport from hydrographic data in the Atlantic (Bryan, 1962; Bryden and Hall, 1980; Roemmich, 1980) indicate that overturning in the vertical-meridional plane is the major mechanism for poleward heat transport. Since this is also true for the models of simple geometry, the same scaling methods can be used to estimate the poleward heat transport. The meridional circulation carries warm surface waters poleward and returns cold deep water toward the equator. Therefore, the poleward heat transport should be proportional to the strength of the overturning. With this highly simplified assumption the heat transport by meridional overturning will be proportional to a scale velocity times a scale depth. Since (7) shows that the scale velocity is proportional to the scale depth, the meridional overturning will be proportional to the square of the scale depth of the thermocline. Results from F. Bryan's and Colin de Verdière's numerical experiments are shown in Fig. 4. F. Bryan's results correspond to 25° N and Colin de Verdière's

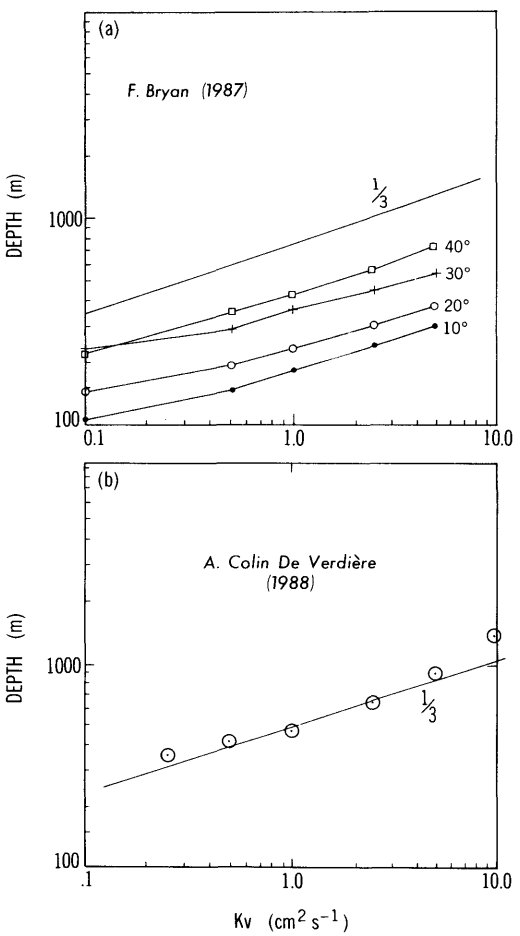

Fig. 3. E-fold depth scale as a function of the vertical diffusivity, K_v, in units of cm^2/s. (a) Experiments of F. Bryan (1987). (b) Experiments of Colin de Verdière (1988). Note that Bryan's experiments include wind which leads to poor agreement with the $\frac{1}{3}$ power law when K_v is small.

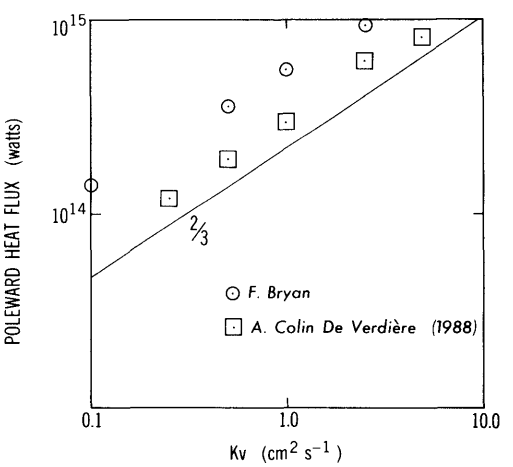

Fig. 4. Poleward heat transport as a function of K_v in units of cm^2/s in the two sets of experiments. Bryan (1987) heat transport values are for 25° N.

results are taken from his Fig. 23. Although Colin de Verdière (1988) felt his best fit for poleward heat transport was for $K_v^{1/2}$, an acceptable fit can also be obtained for $K_v^{2/3}$, which agrees with the simple scaling ideas given above. A more precise test of different scaling laws would require computations over a much greater range of K_v.

The experiments also suggest what a reasonable of K_v should be for a model of this resolution. In Table 2 estimates of poleward heat transport are given from heat balance calculations of the ocean surface made by Simonot and Le Treut (1987) from results of the European Center for Medium Range Weather Forecasting model. The surface heat balance of the ECMWF for 1984 contained a global imbalance of 20 W/m^2. In order to estimate poleward heat transport by ocean currents the authors removed the bias by correcting the evaporative cooling globally.

Results obtained from the European Center model appear to be reasonably stable for different years in the Northern Hemisphere, but differ markedly in the Southern Hemisphere, suggesting that the surface heat balance is quite unsteady from one year to the next. The important point, however, is to compare the order of magnitude of the model poleward heat transport to estimates from data. If we take 500 m as a realistic e-fold depth of the thermocline and 0.5 Petawatts as reasonable value of poleward heat transport for a single basin, Figs. 3 and 4 suggest that a K_v of 0.5–1.0 cm^2/s would appear to be required. A more precise estimate is not practical without considering the actual geometry of the World Ocean in the model and the measurements of poleward heat transport based on in situ measurements planned as part of WOCE (Woods, 1985).

Table 2. *Northward heat transport by ocean currents*

From ECMWF Surface Heat Balance (Simonot and Le Treut (1988) for the year 1984). Estimates for 1985–86 given in parenthesis (Barnier and Simonot, 1990); units are 10^{15} Watts

	Atlantic	Pacific and Indian
25°N	1.1 (0.8)	1.0 (0.8)
25°S	0.4 (0.1)	−2.0 (−0.3)

From F. Bryan's sector experiment at 25°N. Poleward heat transport in the same units

K_v (cm^2/s)	0.1	0.5	1.0	2.5
	0.15	0.38	0.53	0.88

4. Poleward heat transport in a hierarchy of models of increasing resolution

In this section, we review the sensitivity to changes in the horizontal component of diffusion found in models. The parameters of a hierarchy of models of increasing resolution are shown in the three right hand columns of Table 1. The idealized geometry of these three experiments is given in Fig. 5, which shows the time-averaged geostrophic stream lines on a density surface for the eddy-resolving experiment of Cox (1985). Fig. 5 corresponds to the intermediate resolution case in Table 1. Heat and salinity are not included explicitly. Therefore, buoyancy will be a proxy for heat, and we will use the term heat transport and buoyancy transport interchangeably. In the intermediate resolution of Cox (1985) the levels of horizontal viscosity and diffusion are sufficiently low to allow the spontaneous development of mesoscale eddies by baroclinic and barotropic instability. In this model, however, the resolution of $\frac{1}{3}°$ in latitude and $\frac{4}{10}°$ in longitude is barely sufficient to resolve eddies in mid latitudes. The high resolution of Böning (1991) of $\frac{1}{6}°$ in latitude and $\frac{2}{10}°$ in longitude provides a valuable check on any conclusions to be drawn by comparing the low and intermediate resolution results.

The zonally integrated, meridional circulation for the hierarchy of models is shown in Fig. 6. The three cases correspond to a longitude and latitude spacing of approximately 1°, $\frac{1}{3}°$ and $\frac{1}{6}°$. The subgrid scale closure parameters for each case are given in Table 1. An important difference between the highest resolution case and the other two cases is that it has a low random topography on the bottom. This causes some impottant differences in the vertical structure of the variability as discussed by Böning (1989). The very surprising result shown in Fig. 6, however, is how little the overall pattern is changed by increasing resolution and decreasing levels of lateral subgrid scale mixing. The dominant feature in all three cases is a large scale sinking at the poleward wall, compensated by surface inflow and deep outflow toward the

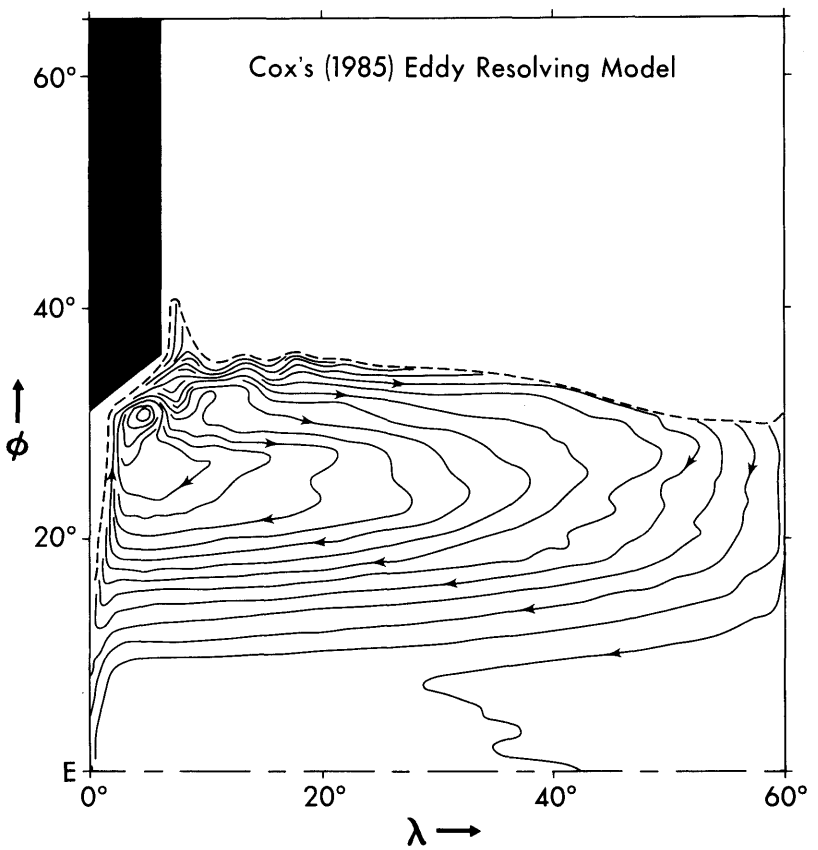

Fig. 5. The time-averaged geostrophic contours on a density surface in the subtropical gyre region (Cox, 1985).

equator. This represents the counterpart of the ocean's thermocline circulation in our simplified model. In all three cases the maximum strength of the meridional overturning is the same, approximately 12 megatons/s (10^9 kg/s). Another common feature of all three resolutions are wind-driven cells near the surface. The strongest surface cell is due to wind-induced upwelling at the equator, balanced by shallow equatorward flow in the upper thermocline. This cell is associated with a powerful poleward flux of heat away from the equator where upwelling causes a maximum ocean uptake of heat through the model ocean surface.

. At middle latitudes there is a partial cancellation between a wind-driven cell with surface flow toward the equator and the main thermohaline cell carrying warm surface water toward the pole. Thus a zonal average makes this cell appear weaker than it really is. The upper branch of the cell is the equatorward Ekman transport below the westerlies at middle latitudes. One of the important roles of this cell is to reduce the poleward transport of heat. Thus the maximum poleward transport of heat in our model is quite near the equator, rather than in middle latitudes as in the atmosphere. Heat balance calculations based on marine observations as shown in Table 1 tend to be consistent with this property of the model.

Several of the diagrams indicate secondary cells in the deep water near the equator. As pointed out by Weaver and Sarachik (1990), these secondary cells are spurious features which disappear when the vertical resolution is increased.

More physical insight on the processes that lead to poleward heat transport is given by plotting the meridional circulation using temperature instead

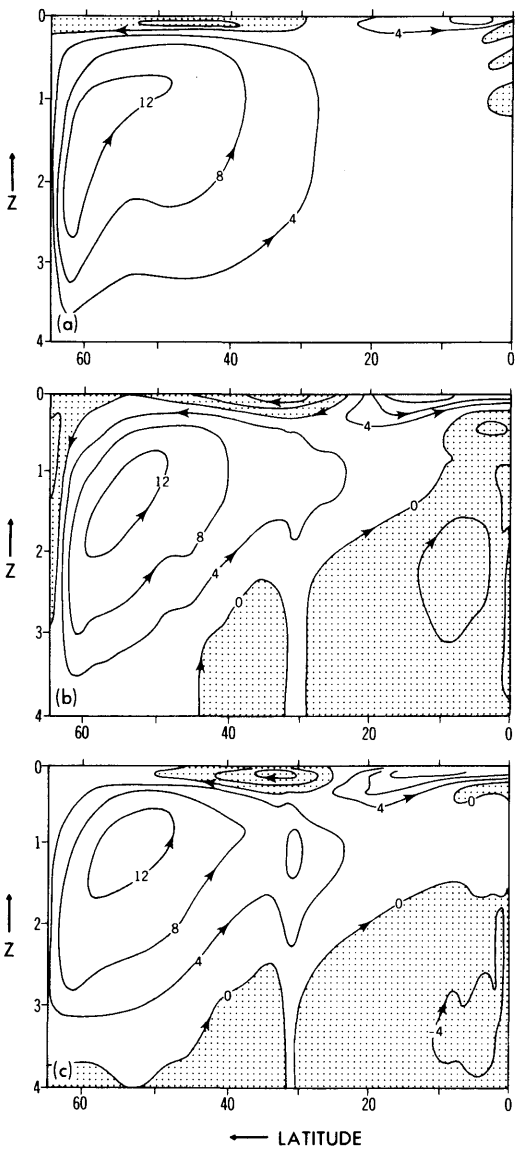

Fig. 6. The transport streamfunction of the total, zonally integrated meridional circulation in units of megatons/s. (a) The low resolution, noneddy-resolving case. (b) The intermediate resolution case of Cox (1985). (c) The highest resolution case of Böning (1991).

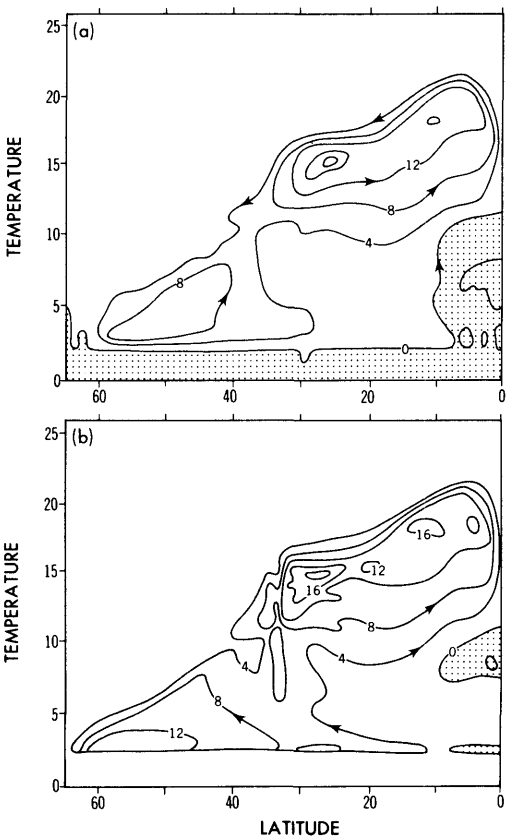

Fig. 7. Transport in the meridional-temperature plane in megatons/s. (a) The intermediate resolution case of Cox (1985). (b) The high resolution case of Böning (1991).

of depth as the ordinate. Time-averaged results are given in Fig. 7 for the two eddy-resolving cases in the hierarchy of models. First let us focus attention on the highest resolution case, Fig. 7b. The units are megatons/s as in Fig. 6. Flow is confined to a triangular area, reflecting the upper boundary condition on temperature. Two main cells circulating in a clockwise manner are evident. The cold cell near the polar wall is easily identified as the main thermohaline cell in Fig. 6. It has an amplitude of 12 megatons/s. The warm cell near the equatorial wall may be identified with the surface wind-driven cell in Fig. 6. It has an amplitude of 16 megatons/s.

The poleward heat transport by each cell is simply proportional to the temperature difference between the poleward moving, warm branch and the equatorward moving, cold branch. It is obvious that the upper warm cell is important in poleward heat transport. This diagram shows that diabatic effects are prominent close to the equator where the thermocline is pushed upward toward

the surface, intensifying the vertical temperature gradient.

At middle latitudes, we can see the signature of the ventilation process very clearly. This feature is in contrast to the picture of meridional circulation in the vertical-meridional plane. Fig. 6 indicates a shallow counterclockwise surface cell in middle latitudes. In Fig. 7, transport through isotherms can only take place in the surface boundary layer or due to subgrid-scale mixing of some kind. At the boundary between the subtropical and subarctic gyres, the western boundary current turns abruptly away from the boundary. In this region, intense convection takes place. Part of this cell lies in the horizontal plane. This is the region where subduction is also a maximum, carrying surface waters down into the thermocline.

Note the large volume of water (over 12 megatons/s) which is carried parallel to the isotherms towards the equator between 30°N and the equator. Motion parallel to the isotherms is consistent with the idea of an ideal fluid thermocline, in which advection dominates mixing processes. In this upper cell diapycnal mixing through density surfaces is principally confined to the surface and to a narrow region below the equator noted previously. These are both regions where a strong mixing would be expected in the real ocean.

Mixing processes are more important in the lower branch of the cold cell in Figs. 8a, b. The cell can be interpreted in terms of the Stommel and Arons (1960) theory for the abyssal circulation. In the Stommel-Arons model upwelling in the ocean interior is associated with a slow poleward flow which is fed by a western boundary current from a polar source region. There is a clear signature of this process. The cold branch of the cell has a nearly uniform temperature indicating relatively rapid transport in a deep boundary current. Sluggish interior poleward flow clearly warms, indicating strong diffusive processes as envisioned in the Stommel-Arons model. This behavior indicates that mixing is of the same order relative as the meridional component of the advection of heat in the lower part of the water column, in contrast to the upper thermocline where the flow is more nearly parallel to the isotherms.

If the meridional circulation is the latitude-temperature plane for the $\frac{1}{3}°$ horizontal resolution case is compared to the highest resolution case shown in Fig. 7b, we see a general similarity. In the lowest resolution case the cells are not as well defined. The ventilation region at the boundary between the subtropical and subarctic gyres is definitely blurred in Fig. 7a. As pointed out in connection with Fig. 6 some of the features in deep

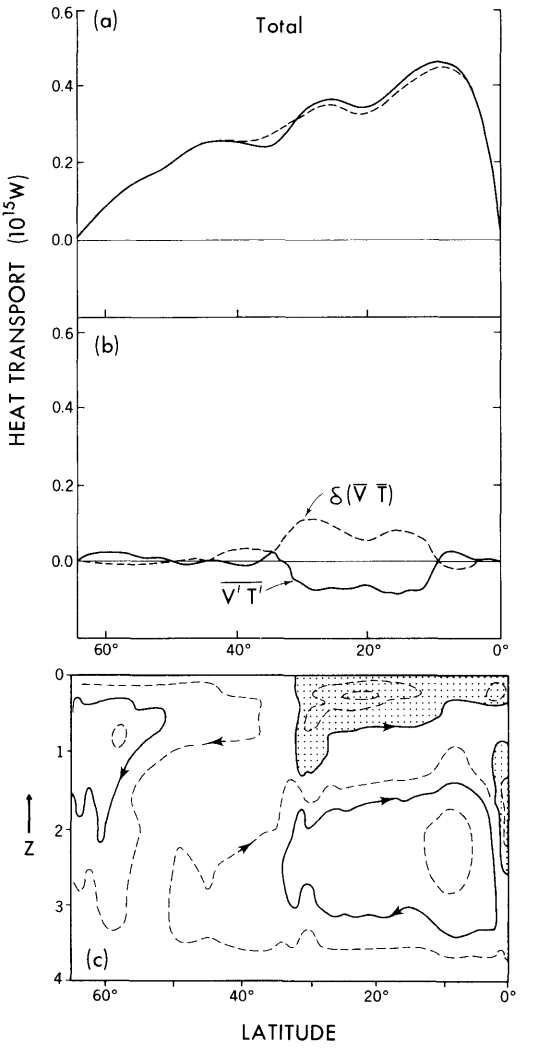

Fig. 8. (a) Poleward heat transport in the eddy-resolving and noneddy-resolving cases of Cox (1985). (b) Poleward transport by transient fluctuations of temperature and meridional velocity and the enhanced poleward transport by changes in the meridional due to higher resolution and the existence of eddies. (c) The difference in meridional circulation between the eddy-resolving and non-eddy resolving case. The contour interval is 1 megaton/s. Reproduced from Bryan (1986).

water near the equator are due to lack of proper vertical resolution in the model.

The similarity in the meridional overturning diagrams for the hierarchy of models shown in Fig. 6 suggests that the poleward heat transport is nearly the same for all three cases. This turns out to be the case. Fig. 8a shows the poleward heat transport as a function of latitude for the eddy resolving model of Cox (1985) and the lower resolution, noneddy-resolving model. The two heat transport curves are nearly identical. In Fig. 8b the poleward heat transport by transient fluctuations is plotted as a function of latitude. In the same diagram the enhanced transport due to the steady state motion is also plotted. Note that the two components nearly cancel out. The mesoscale eddies in the model appear to release potential energy, stir the fluid and mix potential vorticity along density surfaces, but they do not change the poleward transport of heat in the model. The difference in the meridional circulation between the eddy and non-eddy resolving models is given in Fig. 8c which is reproduced from Bryan (1986). We see that in the subtropical gyre region there is a shallow counterclockwise gyre in the high resolution case, which is apparently excited by the eddies. While the eddies transport heat southward, this shallow gyre almost exactly compensates by transporting heat poleward.

5. Discussion and future outlook

Much remains to be done to measure the contribution of ocean circulation to the global heat balance and to construct models that allow a detailed comparison with data. Highly promising work has begun along these lines in connection with WOCE community modelling effort (Bryan and Holland, 1989). However, it is possible to clarify some of the basic issues involved by examining a hierarchy of model experiments of idealized geometry, and increasing resolution that are presently available. These experiments allow an examination of the basic factors which control the thermohaline circulation in a simple context.

The recent parameter studies by F. Bryan (1987) and Colin de Verdière (1988) illustrate the basic importance of vertical mixing in controlling the depth of the thermocline and the intensity of meridional overturning. Application to the real ocean is difficult since only a few direct measurements of vertical mixing are available. What measurements do exist suggest that vertical mixing may be highly variable in space and time. The models suggest that there are certain overall integral constraints on vertical mixing required to drive the thermocline circulation and deepen the thermocline. Inverse modelling with detailed ocean circulation models may be helpful to determine these integral constraints on vertical mixing more accurately for the World Ocean. The assumption of a globally constant vertical diffusivity is rather arbitrary, since it seems likely that vertical diffusion could be quite sensitive to stratification. The effect of stability dependent vertical diffusion has recently been explored by Cummings et al. (1990). The authors conclude in this study that the level of mixing at the base of the thermocline is important for the structure of deep water, but heat transport is largely a function of mixing in the upper part of the water column. It appears that the heat transport results of Bryan (1987) and Colin de Verdière (1988, 1989) still apply, if their values of uniform vertical diffusivity are taken to be representative of the upper thermocline.

The experiments of Cox (1985) and Böning (1989, 1991) provide a hierarchy of models of increasing resolution to determine the sensitivity of poleward heat transport and the thermohaline circulation to the existence of unstable mesoscale eddies. In interpreting the results to the real ocean several caveats must be kept in mind. First the geometry is highly simplified and a condition of mirror symmetry is maintained at the equator. Thus, no heat transport across the equator is allowed in the model. Second, multiple equilibrium states are excluded, since no provision is made for the special boundary conditions which simulate atmospheric coupling by treating temperature and salinity fluxes at the surface in a different way (F. Bryan, 1986). Diagrams of the total meridional overturning integrated zonally indicate the same features in both eddy-resolving and noneddy-resolving models. The poleward heat transport, which is largely associated with this overturning, is very similar in models of roughly one degree latitude and longitude resolution, which do not contain eddies, and models of much higher resolution, which do contain eddies and resolve them in some detail.

Time-dependent eddies in the model indicate

Tellus A-B/43/4-8

a type of behavior which is already well known in connection with the dynamics of the stratosphere (for a review, see Andrews et al., 1987). Observational and modelling studies of the lower stratosphere indicate that in periods when nonadiabatic effects are weak there is a near perfect compensation between poleward transport of heat by correlations between meridional velocity and temperature and the transport of heat by meridional overturning in the time averaged flow. This is exactly what has been found in the eddy-resolving experiments of Cox (1985) discussed in the preceding section. The full "nonacceleration theorem" does not apply to the oceanographic case because of the presence of meridional barriers which allow net zonal pressure gradients. The implications are extremely important for the role of mesoscale eddies in the ocean circulation. However, Fig. 6 shows that the meridional overturning associated with the thermohaline circulation is very much the same for a hierarchy of models, ranging from a noneddy-resolving case to a case where the eddies are very well resolved. Considering the implications for the real ocean we must bear in mind an important caveat. When both temperature and salinity are included in the equaion of state, temperature is no longer uniform on density surfaces. In fact strong temperature gradients on isopycnal surfaces do exist in the polar oceans. In such areas mesoscale eddies can cause a net transport of heat even well below the surface.

As pointed out in Section 1, progress in understanding the Earth's climate requires coupling models of the atmosphere, ocean and the land surface. Climate models must be developed in an iterative process, testing models of each component of the climate system in both a coupled and uncoupled mode. In this paper, we have reviewed results for ocean models for a range of resolution. The focus is on the important role of the ocean in transporting heat poleward from low latitudes. The success of this approach is shedding some insight on the very complex role of mesoscale ocean eddies in the global heat balance suggests that a similar strategy will be useful in studying coupled climate models. In addition to concentrating on building models of the highest feasible resolution, efforts should be made to create a continuous hierarchy of coupled models which can be compared to each other. Isolating the most important elements in climate change is a daunting task. By considering comparable coupled models over a range of resolution, this formidable task may become a little easier.

6. Acknowledgments

It is a pleasure to thank Professor Bolin and his colleagues for a formative and rewarding year spent at the International Meteorological Institute in Stockholm in 1957–58. Thanks are also due to Dr. Claus Böning of the Uiversity of Kiel for permission to cite some of his unpublished work on mesoscale eddies. The author also wishes to thank two anonymous reviewers whose comments were very useful in the final revision.

REFERENCES

Andrews, D. G., Holton, J. R., and Leovy, C. B. 1987. *Middle atmospheric dynamics*, Academic Press, Orlando, FL, 489 pp.

Barnier, B. and Simonot, J. Y. 1990. Net surface heat flux over the North and South Atlantic in 1985–86 from day 1 predictions of the ECMRWF. *J. Geophys. Res. 95*, 13301–13312.

Böning, C. W. 1989. Influence of a rough bottom topography on flow kinematics in an eddy-resolving circulation model. *J. Phys. Oceanogr. 19*, 77–97.

Böning, C. W. 1991. Eddies in a primitive-equation model: sensitivity to horizontal resolution. *J. Phys. Oceanogr.*, in press.

Bryan, F. O. 1986. High-latitude salinity effects and interhemispheric thermohaline circulation. *Nature 323*, 301–304.

Bryan, F. O. 1987. Parameter sensitivity of primitive equation ocean circulation models. *J. Phys. Oceanogr. 17*, 970–985.

Bryan, F. O. and Holland, W. R. 1989. A high-resolution simulation of the wind- and thermohaline-driven circulation of the North Atlantic Ocean. 99–116. Contribution to "*Aha Huliko'a, The Proceedings of the Hawaiian Winter Workshop*, University of Hawaii, Jan 17–20, 1989.

Bryan, K. 1962. Measurements of meridional heat transport by ocean currents. *J. Geophys. Res. 67*, 3403–3414.

Bryan, K. 1986. Poleward buoyancy transport in the

ocean and mesoscale eddies. *J. Phys. Oceanogr. 16*, 927–933.

Bryden, H. L. and Hall, M. M. 1980. Heat transport by ocean currents across 25°N latitude in the Atlantic. *Science 207*, 884–886.

Colin de Verdière, A. 1988. Buoyancy driven planetary flows. *J. Mar. Res. 46*, 215–265.

Colin de Verdière, A. 1989. On the interaction of wind and buoyancy driven flows. *J. Mar. Res. 47*, 595–633.

Cox, M. D. 1985. An eddy resolving numerical model of the ventilated thermocline. *J. Phys. Oceanogr. 15*, 1322–1324.

Cummings, P. F., Holloway, G., and Gargett, A. E. 1990. Sensitivity of the GFDL ocean circulation model to a parameterization of vertical diffusion. *J. Phys. Oceanogr. 20*, 817–830.

Dobson, F., Bretherton, F. P., Burridge, D. M., Crease, J., Krause, E. B., and Vonder Haar, T. H. 1982. *The "cage" experiment: a feasibility study.* World Climate Program, 22, World Meteorol. Organ., Geneva, 95 pp.

Killworth, P. 1989. On the parameterization of deep convection in ocean models. Contribution to *Parameterization of small-scale Processes*, (eds. Peter Müller and Diane Henderson), Hawaii Institute of Geophysics Special Publ., University of Hawaii, 354 pp.

Munk, W. 1966. Abyssal recipes. *Deep-Sea Res. 13*, 707–730.

Roemmich, D. 1980. Estimation of meridional heat flux in the North Atlantic by inverse methods. *J. Phys. Oceanogr. 10*, 1972–1983.

Simonot, J. Y. and Le Treut, H. 1987. Surface heat fluxes from a numerical weather prediction system. *Climate Dyn. 2*, 11–28.

Simonot, J. Y. 1988. *Atlas of ECMWF Surface Fluxes, August 1985–July 1986*, Lab. de Météorologie Dynamique, CNRS, Ecole Normale Supérieure, Paris.

Stommel, H. and Arons, A. B. 1960. On the abyssal circulation of the world ocean, II: An idealized model of the circulation patterns and amplitude in oceanic basin. *Deep-Sea Res. 6*, 217–233.

Weaver, A. J. and Sarachik, E. S. 1990. On the importance of vertical resolution in certain ocean circulation models. *J. Phys. Oceanogr. 20*, 600–609.

Woods, J. 1985. The World Ocean circulation experiment. *Nature 314*, 501–511.